NOTES AND CORRESPONDENCE

On the Effects of Filtering on Convective-Core Statistics

MARGARET A. LEMONE AND TAE Y. CHANG*

*National Center for Atmospheric Research,** Boulder, Colorado*

CHRISTOPHER LUCAS

Department of Meteorology, Texas A&M University, College Station, Texas

21 September 1993 and 10 March 1994

1. Introduction

The analysis of convective events north of Australia during the Equatorial Monsoon Experiment (EMEX) by Lucas et al. (1994a) reinforces accumulating evidence that convective cores over the tropical ocean are surprisingly weak, with small diameters and vertical velocities. A convective updraft core is defined as having a vertical velocity $w \geq 1$ m s^{-1} for at least 500 m, and a downdraft core is defined analogously. With the EMEX study, such weak events have been documented over much of the tropical oceans—the eastern Atlantic in the Global Atmospheric Research Program's Atlantic Tropical Experiment (GATE) (Zipser and LeMone 1980; LeMone and Zipser 1980, hereafter referred to as ZL and LZ), the western Atlantic and Gulf of Mexico in hurricanes (Jorgensen et al. 1985), and the subtropics during the Taiwan Area Mesoscale Experiment (TAMEX: Jorgensen and LeMone 1989).

Such statistics are important because they provide a "reality check" for convective parameterizations that involve cloud diameter, vertical velocity, or mass flux (e.g., Arakawa and Schubert 1974, Cheng 1989a,b), or for one-dimensional cloud models (e.g., Ferrier and Houze 1989, which lists a number of earlier examples). The parameterization scheme recently described by Donner (1993) is partially based on convective-core statistics.

Zipser and LeMone (1980) argued that GATE cores were surprisingly small and weak because our expectations had been defined by studies over land such as the Thunderstorm Project (Byers and Braham 1949).[1] Lucas et al. (1994a) noted two factors that in combination could explain the difference in core strengths. First, buoyancies at lower levels tend to be much higher over heated land than over the oceans. This is mainly the result of differences in thermal buoyancy, water-loading being about the same (if not larger) for continental situations. This would tend to make stronger continental updrafts at the lower levels sampled (usually less than 6 km), even if the convective available potential energies (CAPEs) were comparable. And second, updraft diameters seem to be larger over land, which would reduce entrainment. Clearly, the validity of the second argument depends on the validity of the diameter estimates in both places.

Yet there has been reason to question the reported small size of oceanic core diameters. Zipser and LeMone and LZ defined updraft cores as having continuous vertical velocity of 1 m s^{-1} or greater for 500 m or more. Recognizing that aircraft do not necessarily intercept the center of a vertical velocity event, Jorgensen et al. (1985) noted that random sampling of a circular core with diameter d would yield an average diameter of $(\pi/4)d = 0.78d$, hardly a major effect. However, the superposition of smaller-scale turbulence on the convective core signal could yield artificially small cores, by producing w spikes under 1 m s^{-1}. These spikes would artificially separate the expected large cores into two or more small cores under the ZL/LZ criteria, as shown for core a in Fig. 1. To investigate this potential source of bias, we decided to do a side-

* Current affiliation: Department of Mechanical Engineering, University of Colorado.

** The National Center for Atmospheric Research is sponsored by the National Science Foundation.

Corresponding author address: Christopher Lucas, Department of Meteorology, Texas A&M University, College Station, TX 77843-3150.

[1] Zipser and LeMone's arguments are summarized in Lucas et al. (1994b).

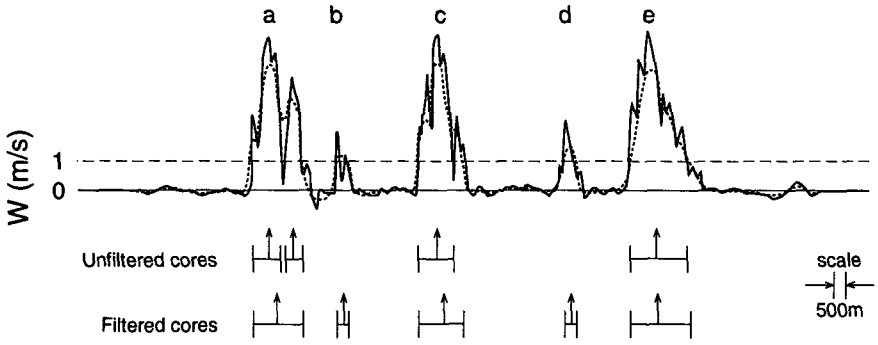

FIG. 1. Schematic showing the effect of filter in Fig. 2 on events counted as convective cores: **a** denotes *old core–old core merger,* two cores in unfiltered dataset being merged into one core in the filtered data; **b** denotes *small core–small core merger,* a new core forming out of two cores too small to be counted in the unfiltered data; **c** denotes *old core–small core* merger, in which a core in unfiltered data is merged with a core too small to be identified in unfiltered data to make a single, larger core; **d,** a core too small to be identified in unfiltered data becomes a core in the filtered data due to broadening; and **e,** an old core becoming broader.

by-side analysis of filtered and unfiltered vertical velocity data while investigating the EMEX convective cores.

We show that while the filtering procedure occasionally merges smaller cores into larger ones, the rarity of mergers of two "unfiltered" cores into one "filtered" one and the inclusion of small cores formerly excluded by the 500-m cutoff leads to only a small increase in the apparent diameter. Mean vertical velocity is slightly reduced by both core mergers and inclusion of the small, generally weak events. Mass flux is virtually unaffected, since it is the product of diameter, which is increased by filtering and mean vertical velocity, which is decreased by filtering. However, there is a very slight increase, since both core mergers and the addition of small events increases the number of points with positive vertical velocity. Maximum vertical velocities are not strongly affected but are mostly decreased by the introduction of small cores by the filter. The effects of filtering on downdraft cores is similar.

The data collection and analysis procedures are discussed in section 2. Filtered and unfiltered data are compared in section 3, and conclusions are summarized in section 4.

2. Data collection and analysis

a. Data collection

The data used in this study were collected by the NOAA P3 and the NCAR Electra during EMEX. The flights were designed to document mesoscale convection. The aircraft flight patterns differed somewhat—the P3 patterns were zigzags designed to sample convergence with the Doppler radar, while the Electra flew long lines normal to convective bands to sample data in situ. Although the difference in the strategies could have affected the samples, there was no obvious effect: both aircraft documented significant convection.

Vertical velocities were found by subtracting the aircraft velocity relative to the ground from the air velocity relative to the aircraft. The procedures are described in Jorgensen and LeMone (1989) and in Lenschow (1972). The P3 data were sampled once a second, and the Electra data at 20 s^{-1} in order to sample turbulence. Thus, the Electra data were averaged to once per second to remove biases due to differing instrument response and sampling rate.

b. Data analysis procedure

We selected 338 straight and level flight legs from the two aircraft for analysis, based on comparison of flight tracks to radar composites by Gamache et al. (1987). These legs were not screened for active convection as were those used in Lucas et al. (1994a). However, there is a considerable overlap, and the results of the unfiltered analyses are similar. This is probably because the legs in less active cloud had few or no cores.

Filtering was done with a Graham (1963) filter because of the facility with which the filter response function can be varied. The response function (Fig. 2) is designed to have a response near unity at frequencies less than the cutoff frequency f_c and near zero at frequencies greater than the terminating frequency f_t, with a cosine fall off between f_c and f_t. The closeness to the ideal response increases with the number of weights, N: N is an odd number; the weights are symmetrical about a central weight W_0, given by

$$W_0 = (f_c + f_t)\Delta t,$$

where f_c and f_t are the cutoff and terminating frequencies, and Δt is the sampling interval (in this case 1s).

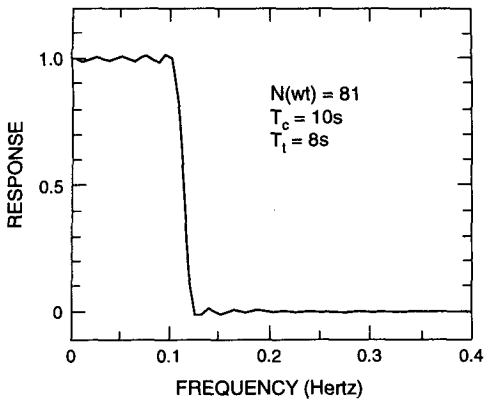

FIG. 2. Response function of Graham filter used. Falloff approximates a cosine. The periods T_c and T_t correspond to cutoff and terminating frequencies $f_c = 0.1$ and $f_t = 0.125$.

The ith weight is a time interval $\pm i\Delta t$ from the central weight. Then, for i from 1 to $\frac{1}{2}(N-1)$,

$$W_i = 0.5\,\frac{\sin(2\pi\Delta t f_t i) + \sin(2\pi\Delta t f_c i)}{i[1 - 4(i\Delta t)^2(f_t - f_c)^2]}.$$

The weights W_i are then normalized by their sum.

After much experimentation, we selected cutoff and terminating frequencies corresponding to periods of 10 and 8 s, which includes cores more than ~500 m (the cutoff length for cores) across, and excludes updrafts less than ~400 m across. We selected $N = 81$ to ensure a reasonable-looking response curve. Since the filter is symmetric, 40 weights are included on either side of the point of interest. Hence, 40 seconds at both ends of each flight leg cannot be filtered. The vertical velocities at these points are set to zero.

The filtered and unfiltered time series were then examined for the presence of cores, using identical procedures to ensure that the only differences in core properties were due to the filter itself. Prior to this, as mentioned in Lucas et al. (1994a), the measured mean vertical velocity, assumed to be a bias, was subtracted out. These means were calculated for each aircraft from sequences of consecutive or near-consecutive unfiltered flight legs at the same altitude. Groups of legs were used because EMEX flight legs were often much shorter than those flown in GATE, and typically spent less time in undisturbed air. After subtraction of the mean, the end times for the positive vertical velocity events with values greater than 1 m s^{-1} for 500 m or more were identified as cores and recorded along with their diameter (product of airspeed and the time interval in a core), maximum vertical velocity (w_{max}), and average vertical velocity ($\bar{w}$). For downdrafts, the same analysis was done after multiplying the time series by -1. Pressure and temperature were recorded for each leg to obtain density for mass-flux calculations.

Setting $w = 0$ for the 40 points at the ends of each "filtered" leg eliminated some cores from the filtered data, and cut off portions of others. For these cases, the corresponding cores in the unfiltered dataset partially or completely lose their "filtered" counterparts. Thus, *all cores—filtered and unfiltered—that overlapped with the 40 points at either end of the flight leg had to be eliminated* from the dataset. This was done in two steps. First, such cores were eliminated from each dataset objectively. After this was done, we examined the lists of filtered and unfiltered cores to eliminate filtered cores whose unfiltered counterparts had been removed by the objective procedure, and vice versa. While this procedure eliminated some "good" cores that would have otherwise been analyzed, it ensured that we were isolating effects due to the filter itself.

The cores based on filtered and unfiltered data were then analyzed in exactly the same way as done by ZL and LZ. Distributions of the events were plotted as a function of w_{max}, $\bar{w}$, diameter, and $\log_{10}$ mass flux. As before, mass flux is the product of density, distance, and vertical velocity—a kind of mass flux per unit length. In this way we avoid any assumption of core geometry. Cumulative distributions of the same parameters were plotted on log-probability paper to determine the median or 50% value and the value defining the top 10% of the cores (the 10% value). These values were then compiled for three different height intervals used in ZL and LZ—0.7 to 2.5 km, 2.5 to 4.3 km, and 4.3 to 8.1 km. We chose not to include data at lower levels because there were too few legs flown by the aircraft used in this analysis. It should be noted that the filtered data are used *only* for determining core times: the unfiltered data are used subsequently. Thus, if the filtering procedure fails to change the individuals in the population through introducing new cores or merging old ones, the distribution for w_{max} should be unaltered.

c. *Expected effects of filtering*

To facilitate discussion of the results, we briefly summarize the effects that filtering should produce. From event (a) in Fig. 1, we expect the filter to merge cores already counted in the statistics. Because the cores were already counted before the filtering procedure, we call these *old core–old core* mergers. This adds a larger diameter to the distribution in the place of two smaller ones and eliminates the lower value of maximum vertical velocity w_{max}. The effect on the distribution of w_{max} depends on the two magnitudes. Events could be eliminated from either the high or low end. The average vertical velocity $\bar{w}$ is usually reduced by inclusion of data between the old cores.

The core(s) labeled **b,** like **a,** represent(s) a core merger resulting from filtering, but with a different effect. Here, the two events merged are too small to be counted as cores before the filtering procedure, but the merged core "makes the cut." Hence we call this a *small core–small core* merger. The net effect is a decrease in average diameter, and more events at the

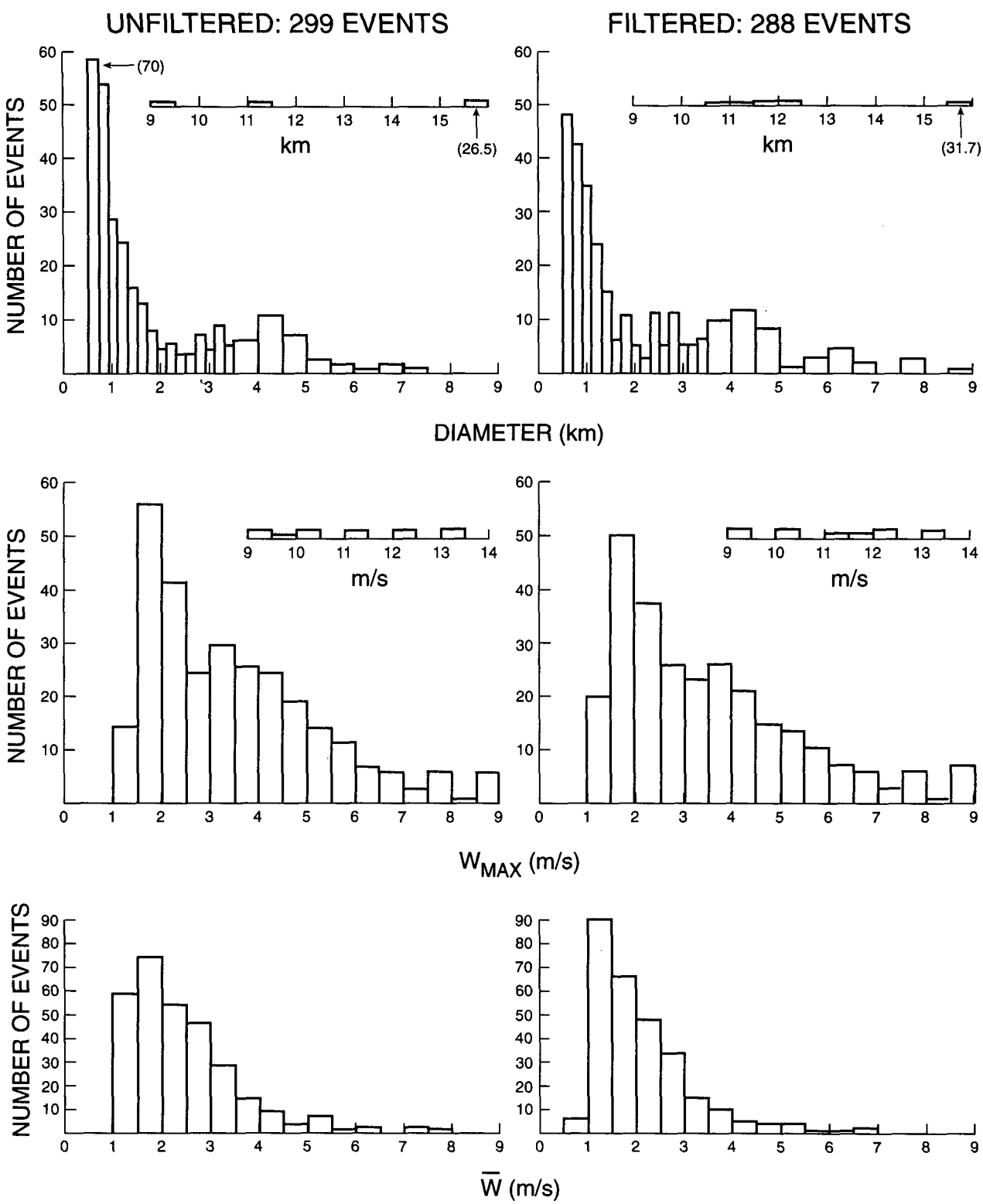

FIG. 3. For convective updraft cores from 4.3 to 8.1 km (top) diameter distribution, (middle) distribution of w_{max}, (bottom) distribution of $\bar{w}$. Cores identified from unfiltered data (left) and filtered data (right).

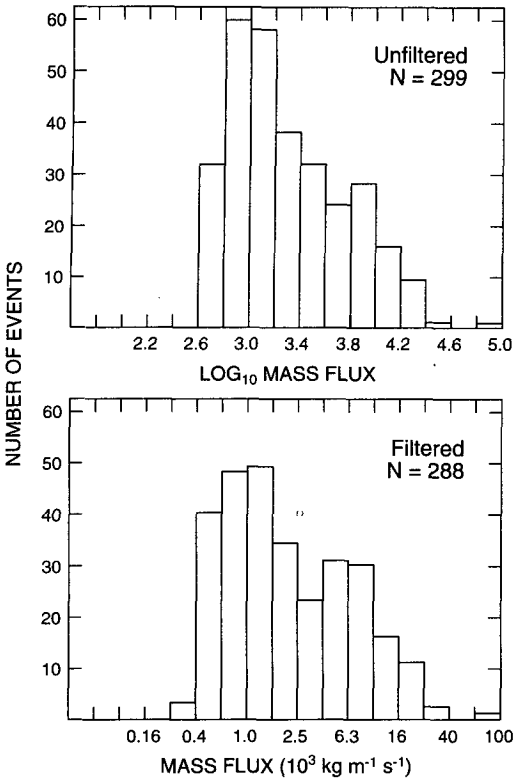

FIG. 4. Distribution of mass flux for updraft cores of Fig. 3.

small end of the distribution. Since smaller cores *tend* to have smaller vertical velocities, this usually adds lower values of $\bar{w}$ and w_{max} to the distribution, but not always!

The core(s) labeled **c** is an intermediate case—the merger between a core appearing in the unfiltered data and a core too small to be counted in the unfiltered data. This *old core–small core* merger tends to increase the diameter. Its effect on w_{max} could go either way, but $\bar{w}$ is usually reduced from the inclusion of data with vertical velocity less than 1 m s^{-1} as well as the typically lower vertical velocity air in the small core.

Cores **d** and **e** represent *broadening* by the filter. This usually increases "old" core diameters by a few hundred meters (corresponding to a second or two), as in **e.** It can also introduce new cores too small to meet the 500-m criterion before filtering, adding small-diameter cores like **d** to the distribution. The net effect on diameter depends on whether **d** or **e** dominates. Average vertical velocity $\bar{w}$ is reduced by introduction of weak updraft at the edges of "old" cores and the usually weak vertical velocities with the small cores introduced by filtering. Of the two mechanisms, only **d** affects w_{max} by adding new individuals—usually with small values.

3. Results

a. *Sample distributions*

We illustrate the effects of filtering by considering the dataset for updrafts at 4.3 to 8.1 km since this dataset includes the largest number of events—299 updraft cores for the unfiltered data and 288 cores for the filtered. The diameter, maximum vertical velocity, and mean vertical velocity distributions appear for the updraft cores in Fig. 3. Filtering reduces the number of events at this level—the effect of old core–old core mergers—but the general shape of the distributions is preserved. The distribution for diameter is most profoundly affected by filtering, as would be expected. The 10% core diameter is increased from 3.9 to 4.7 km. However, the 50% value only increases from 1.1 to 1.3 km. Old core–old core mergers probably account for the greater diameter increase for the larger cores. Filtering introduces six individuals with $\bar{w}$ less than 1 m s^{-1} to the $\bar{w}$ distribution, the expected effect of including data with $\dot{w} < 1$ m s^{-1} between formerly separated cores. Least affected is the w_{max} distribution. This is not surprising, since the filtered core times are applied to unfiltered data.

Note that six updraft cores actually have a value of $\bar{w}$ under the 1 m s^{-1} threshold. This occurs because the average is based on unfiltered data while the core times are based on filtered data: had we used filtered data in the averaging, these cores would have all had values of $\bar{w}$ slightly greater than 1. These cores all had diameters less than 1 km. Most, if not all, of these events, were probably introduced by filtering—either through merging of small cores or through broadening a small core enough to meet the 500-m criterion.

Figure 4 shows the distribution of mass flux by updrafts at 4.3–8.1 km. Again, the general shape of the distribution is preserved. Introduction of small cores at the low end of the spectrum and merging or broadening involving old cores broadens the filtered spectrum slightly. The 50% and 10% values of mass flux are virtually unaffected because of the counteracting effects by filtering on diameter and mean vertical velocity.

b. *The effect of filtering on core properties*

Figure 5 shows profiles of the number of events, and 10% and 50% values of diameter, w_{max}, and $\bar{w}$, for filtered (dashed line) and unfiltered (solid line) updrafts and downdraft cores.

1) NUMBER OF EVENTS N

Typically, filtering changes the number of cores. Filtering usually increases the number of cores in the sample, indicating that introduction of new, small cores dominates the loss of individuals in the population through old core–old core mergers. A significant de-

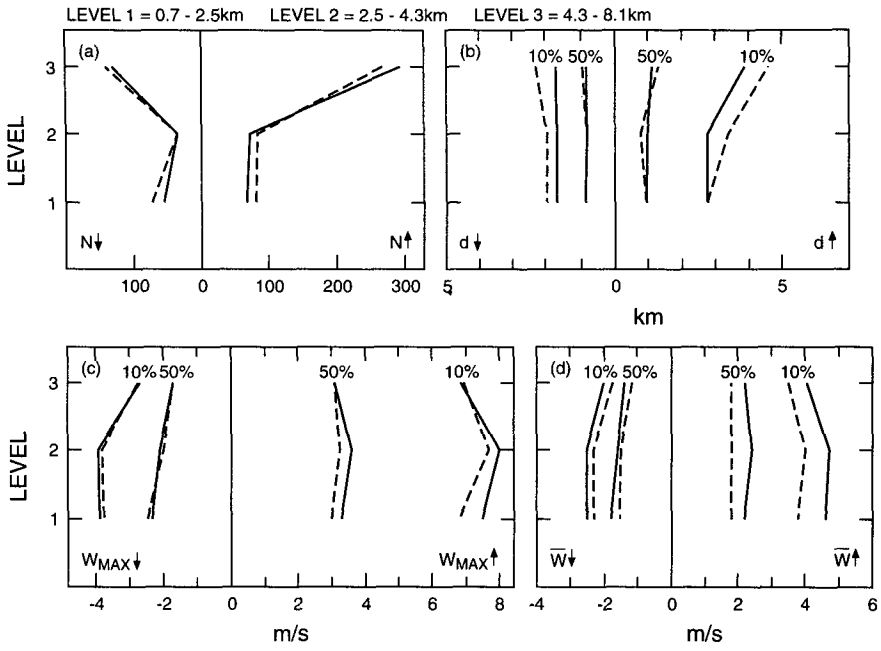

FIG. 5. Profiles of (a) number of events N; 50% and 10% values for (b) diameter d, (c) maximum vertical velocity w_{max}, and (d) mean vertical velocity $\bar{w}$, for cores identified using filtered (dashed line) and unfiltered (solid) data.

crease in core number due to filtering is seen only for updrafts at 4.3–8.1 km; the associated dominance of mergers is reflected in the increase in diameter at this level. A small effect on the number of samples does not guarantee a small effect on the results—note that the percentage increase in diameter for the 10% downdraft cores at 2.5–4.3 km is fairly significant in spite of a small change in N.

2) DIAMETER d

The filtered data show an increase in the 10% values for most cases, the combined effect of smoothing-induced core broadening and mergers. At 2.5–4.3 km and 4.3–8.1 km, the diameter of 10% cores was increased by 20% to 25% for both updrafts and downdrafts. The fact that this effect is not universal indicates that broadening events and old core–old core mergers do not always occur in sufficient number to offset the effect of new cores introduced at the small end of the distribution. For example, filtering produces no significant difference in the diameter of 10% updraft cores at 0.7–2.5 km; and at 2.5–4.3 km, the 50% diameter is smaller for the updraft cores based on filtered data. In general, the apparent diameter increase from filtering increases with height.

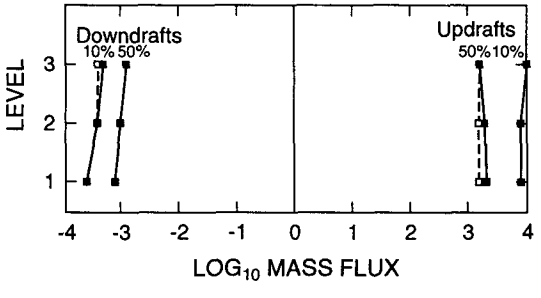

FIG. 6. As in Fig. 5 but for mass flux.

3) MAXIMUM VERTICAL VELOCITY w_{max}

The effects of filtering are mixed, but the values based on filtered data are usually lower, with the largest effect (about 10%) for the updraft cores at 0.7–2.5 km. This probably is due to the introduction of small, weak events; but elimination of points at the "high" end of the distribution by the merging of two strong individuals could also be a factor. When w_{max} is greater for the filtered data, mergers could have eliminated some of the weaker (low w_{max}) cores, or small-diameter events with large w_{max} could have been introduced. The average ratio of filtered to unfiltered values is 0.97 for both 50% and 10% cores.

4) AVERAGE VERTICAL VELOCITY $\bar{w}$

From Fig. 1, we would expect filtering to decrease values of $\bar{w}$ and hence the 50% and 10% values: core mergers and introduction of new cores normally introduce more low w values than high ones, and core broadening almost always introduces lower values of

w. Thus it is not at all surprising that filtering lowers the 50% and 10% values of $\bar{w}$ by as much to 15%–20%. The average ratios of filtered to unfiltered $\bar{w}$ are 0.84 for the 50% values, and 0.87 for the 10% values.

5) MASS FLUX

Figure 6 shows the profiles of 10% and 50% values for filtered and unfiltered data. From the foregoing, we would not expect much effect, since filtering increases diameter but decreases $\bar{w}$; but we would expect a slight increase in total mass flux because more data with positive vertical velocity are included in the sample. This is confirmed by Fig. 6. The differences between the filtered and unfiltered values of the 10% mass flux are mostly not detectable on the graphs. Actual ratios of filtered to nonfiltered values average 1.01, five of six values are over 1; one value is 0.99. For the median, the filtered:nonfiltered ratios are less than one for half the cases. This reflects the introduction of a number of small events; indeed, in all three cases (the one not obvious from the figure is for the downdrafts at 0.7–2.5 km), the number of events is increased by filtering.

4. Summary and conclusions

The effects of filtering vertical velocity data to identify updraft and downdraft cores were noticeable but smaller than expected. Updraft cores are defined as having vertical velocity >1 m s^{-1} for at least 500 m, and downdraft cores are defined analogously; so the filter was designed to eliminate events with less than a 500-m apparent diameter.

Thus median and 10% core diameters were increased by 20%–25% at most, with the larger increases at higher levels (fewer small events). The 50% and 10% values of $\bar{w}$ were decreased by up to 15%–20% at all levels, since the filtering effects involving both broadening and merging tend, on average, to introduce times with smaller vertical velocities. The maximum vertical velocity is changed only by changing the individual events in the distribution, but changes are detectable. At the lower levels, where many small, weak cores are introduced by filtering, w_{max} for the updraft cores is lowered by up to around 10%. Mass flux is changed the least, since diameter and mean vertical velocity respond to filtering in opposite ways. However, the filtering procedure increases total mass flux slightly due to inclusion of more upward moving air into the sample.

The perhaps surprisingly small effect stems from the fact that the filter introduces many new small events to the dataset, counteracting the increase in the number of large events through mergers of adjacent cores. Viewing the high-frequency "turbulence" as interfering with proper core identification, we could say that missing these small events is just as bad as artificially splitting the big events. We assert that any good-quality low-pass filter designed to eliminate events smaller than 500 m in scale would give similar results: differences in the response function from that of Fig. 2 would change the details but not the basic conclusions.

Acknowledgments. The LeMone and Chang research was supported by NCAR and by National Science Foundation Grant ATM 9215507; Lucas was supported by National Science Foundation Grant ATM 9019757 and by National Aeronautics and Space Administration Grant NAG5-1569. The authors wish to thank Ed Zipser for many useful discussions; Jim Fankhauser and Jim Dye made useful comments on the manuscript.

REFERENCES

Arakawa, A., and W. H. Schubert, 1974: Interaction of a cumulus cloud ensemble with the large-scale environment. Part I. *J. Atmos. Sci.*, **31,** 674–701.

Byers, H. R., and R. R. Braham, 1949: *The Thunderstorm Project.* U.S. Weather Bureau, U.S. Dept. of Commerce, 287 pp. [NTIS PB234515.]

Cheng, M.-D., 1989a: Effects of downdraft and mesoscale convective organization on the heat and moisture budgets of tropical cloud clusters. Part I: A diagnostic cumulus ensemble model. *J. Atmos. Sci.*, **46,** 1517–1538.

——, 1989b: Effects of downdraft and mesoscale convective organization on the heat and moisture budgets of tropical cloud clusters. Part II: Effects of convective-scale downdrafts. *J. Atmos. Sci.*, **46,** 1540–1564.

Donner, L. J., 1993: A cumulus parameterization including mass fluxes, vertical momentum dynamics, and mesoscale effects. *J. Atmos. Sci.*, **50,** 889–906.

Ferrier, B. S., and R. A. Houze Jr., 1989: One-dimensional time-dependent modeling of GATE cumulonimbus convection. *J. Atmos. Sci.*, **46,** 330–352.

Gamache, J. F., F. D. Marks, and R. W. Burpee, 1987: EMEX data report: The Equatorial Mesoscale Experiment. AOML/HRD Rep., 98 pp. [Available from Prof. Robert A. Houze, Dept. of Atmospheric Sciences, University of Washington, AK-40, Seattle, WA, 98195.]

Graham, R. J., 1963: Determination and analyses of numerical smoothing weights. NASA Tech. Rep. TR-179, 28 pp.

Jorgensen, D. P., and M. A. LeMone, 1989: Vertical velocity characteristics of oceanic convection. *J. Atmos. Sci.*, **46,** 621–640.

——, E. J. Zipser, and M. A. LeMone, 1985: Vertical motions in intense hurricanes. *J. Atmos. Sci.*, **42,** 839–856.

LeMone, M. A., and E. J. Zipser, 1980: Cumulonimbus vertical velocity events in GATE. Part I: Diameter, intensity and mass flux. *J. Atmos. Sci.*, **37,** 2444–2457.

Lenschow, D. H., 1972: The measurement of air velocity and temperature using the NCAR Buffalo aircraft measuring system. NCAR-TN-EDD-74, 39 pp. [Available from NCAR, P.O. Box 3000, Boulder, CO 80307.]

Lucas, C., E. J. Zipser, and M. A. LeMone, 1994a: Vertical velocity in oceanic convection off tropical Australia. *J. Atmos. Sci.*, **51,** 3183–3193.

——, ——, and ——, 1994b: Convective available potential energy in the environment of oceanic and continental clouds: Correction and comments. *J. Atmos. Sci.*, **51,** in press.

Zipser, E. J., and M. A. LeMone, 1980: Cumulonimbus vertical velocity events in GATE. Part II: Synthesis and model core structure. *J. Atmos. Sci.*, **37,** 2458–2469.